International Journal on Interactive Design and Manufacturing (IJIDeM)
https://doi.org/10.1007/s12008-018-0508-2

ORIGINAL PAPER

Mechanical efficiency prediction methodology of the hypocycloid gear mechanism for internal combustion engine application

Mostafa A. ElBahloul[1] · **ELsayed S. Aziz**[1,2] · **Constantin Chassapis**[1]

Received: 12 July 2018 / Accepted: 28 August 2018

Abstract
Mechanical friction power loss is one of the main concerns in the internal combustion engine (ICE) systems. The piston-rod assembly and the complex motion of the connecting rod are the largest source of engine friction. A significant reduction in these losses can be achieved with ICE systems incorporating the hypocycloid gear mechanism (HGM), which ensures that the piston-rod assembly reciprocates in a perfect straight-line motion along the cylinder axis to eliminate the piston side load. This paper investigates the feasibility of an enhanced HGM for the design and development of ICE applications. It incorporates designing the planetary crank gearing system to satisfy the design specifications of ICE using the standard design procedures provided by AGMA. This is followed by building the friction model for the interacting components of the HGM engine through developing the mathematical model for the friction power loss of the internal gear train meshes, rolling bearings, and sliding bearings. The total friction power losses of the HGM engine are calculated and compared with the friction model of the conventional crank-slider engine that has been developed by Sandoval and Heywood (An Improved Friction Model for Spark-Ignition Engines. SAE Technical Paper 2003-01-0725, 2003). The comparison results show the feasibility of using the HGM for ICE applications with minimized engine friction power losses and hence higher mechanical efficiency.

Keywords Hypocycloid · Internal gears · Friction modeling · Power loss · Internal combustion engines · Mechanical efficiency

1 Introduction

The kinematics of ICE has utilized the traditional crank-slider mechanism for its simplicity and for this reason; it has remained almost unchanged since its introduction. However, in the past and even nowadays, different mechanisms have been studied and analyzed because of their advantages over the crank-slider mechanism and the possible positive enhancements that can be achieved for better engine performance and higher efficiency. As an example for this effort is the sinusoidal engines, so named because the mechanisms incorporated allows the piston to move in sinusoidal straight-line motion. One of the mechanisms utilized with sinusoidal engines is the planetary gear train mechanism. This mechanism is kinematically recognized as hypocycloid mechanism, since *Hypocycloid* is the term that describes the basic kinematic principle involved. Some literatures prefer using the term *Cardanic* but it is the same principle.

One main concern of using the conventional crank-slider mechanism is the piston assembly friction that was reported to constitute 40–55% of the entire engine friction [2, 3]. The main reason for such high friction is the complex motion of the connecting rod that, from the piston's end, generates a large thrusting force against the cylinder wall. At the crank-pin end, it generates lateral forces pushing the crankshaft sideways, as shown in Fig. 1. The side thrusting was reported to cause wear to the piston ring assembly and cylinder wall (piston slap), as well as an increase in the frictional losses [4, 5]. These losses have a significant effect on the engine,

✉ Mostafa A. ElBahloul
melbahlo@stevens.edu

ELsayed S. Aziz
eaziz@stevens.edu

Constantin Chassapis
cchassap@stevens.edu

[1] Department of Mechanical Engineering, Schaefer School of Engineering and Science, Stevens Institute of Technology, Hoboken, NJ 07030, USA

[2] Production and Mechanical Design Engineering Department, Faculty of Engineering, Mansoura University, Mansoura 35516, Egypt

Published online: 31 August 2018

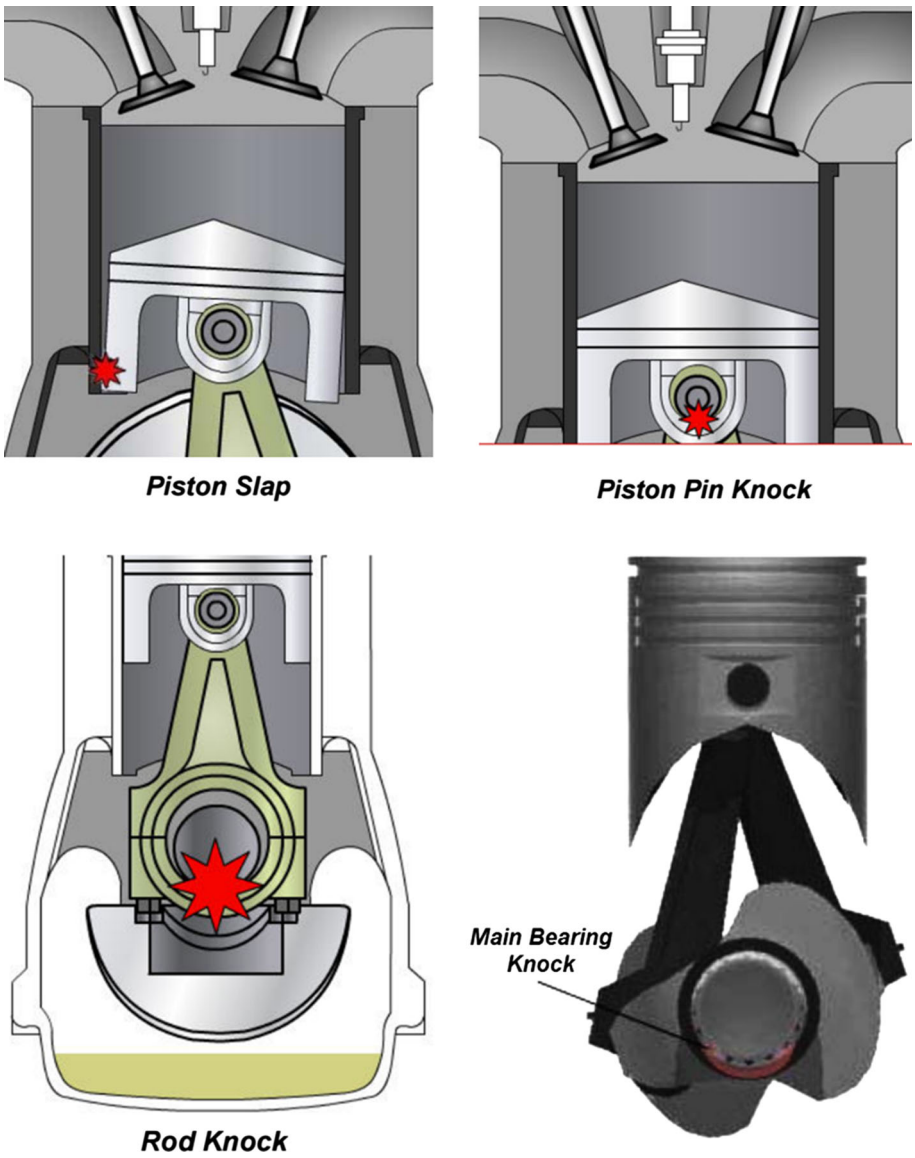

Fig. 1 Common mechanical faults with conventional engines

so minimizing them would improve engine performance and enhance the vehicle fuel economy.

On the other hand, a hypocycloid mechanism provides several characteristics that makes it attractive for ICE applications [6–8]. The piston motion to start with is purely sinusoidal relative to crank rotation angle, as opposed to the motion produced by a conventional crank-slider mechanism. This would be beneficial for achieving perfect engine balance for any number of cylinders. The straight-line motion of the piston and connecting rod would eliminate the need for the wrist pin bearing which allows for a very short piston without concerns of chocking occurrence. In addition, this motion should eliminate the piston side thrusting into the cylinder walls that would allow for minimizing piston friction losses, eliminating the piston skirt, and preventing the piston slap occurrence even with large piston-cylinder clearance. The elimination of side thrusting forces would also result in increased engine output power, which would allow for smaller engine displacement, hence smaller cylinder length, with the advantages of lower engine weight, size, and cost.

The mechanism characteristics briefly mentioned above show that the HGM engine might have significant advantages over the conventional crank-slider engine. Despite these advantages, the mechanism would be beneficial only if it can be shown to handle loads and speeds for a modern ICE, and to be manufactured within a reasonable size at a reasonable cost. Several attempts were carried out for applying this concept with ICE applications; some of these attempts are briefly presented below.

A comprehensive analysis for the basic HGM engine design was carried out by Karhula [9] under two applications,

air pumps and four stroke engines, to assess the old cardan gear mechanism (basic HGM) against the conventional crank-slider mechanism. The study showed a comprehensive investigation and a comparison between the two mechanisms in terms of the kinematic characteristics, the inertial forces included, thermodynamics, torques and power output, the total frictional losses, and total mechanical efficiencies. It was concluded that the cardan mechanism is worth utilizing for better energy savings due to the good mechanical efficiency achieved, and preliminary design guidelines to be used for cardan gear machines was provided. A few years later, the engine proposed by Wiseman Technologies Inc. [10] incorporating the basic HGM arrangement was investigated where Lotus Engine Simulation software was used for modeling engine specifications and simulating engine performance. The simulation results were later compared with experimental tests carried on a prototype (*WHE alpha*) for the engine. The results showed a confirmation between simulations and the experimental testing, and the resulting engine performance showed promising results for torque and power output as compared to the conventional crank-slider engine. In addition, further simulations on the diesel four-stroke version of the engine were done with some analysis on the fuel efficiency.

The fact that the connecting rod's motion is in a perfectly straight-line was made use of where the lower portion of the cylinder was utilized as a second working chamber. Badami and Andriano [11] ran experimental tests on two prototypes, one for a double acting reciprocating compressor and the other for two-stroke spark ignition engine. Despite the fact that the compressor results showed large increase in the mechanical efficiency as compared with single acting compressors, some difficulties appeared with the two-stroke spark ignition engine, particularly with the sealing between lower chamber and the crank case, in addition to the design and construction of gears and bearings, and suggested lubrication mechanism. Rucker [12] applied a similar concept but to a parallel combustion two-stroke engine. The two chambers in the working cylinder were connected with combustion chambers external to the working cylinder where the new cycle consisted of five distinct functions, each defined by a full piston stroke without the function overlap common in existing two-stroke engine. Therefore, this idea combined most of the advantages of four stroke engine and external combustion engine into a two-stroke engine.

An enhanced version of the HGM engine [13, 14] was introduced recently with a main objective of improving the combustion characteristics. It was aimed for improving the efficiency of the internal combustion engine through allowing for true constant volume combustion, which in turn would lead to higher work output. The simulations carried out for the enhanced design were shown to achieve higher in-cylinder pressure, near constant volume combustion at top dead center (TDC), and more air charge time at bottom dead center (BDC) as compared to the conventional crank-slider engine. This came along with the improved performance over even the basic HGM engine in kinematic characteristics and torque output. In continuation for the work done on HGM, this study is aiming for modeling and analyzing the frictional losses of the components incorporating the HGM engine, then comparing the performance of the enhanced HGM design with the conventional crank-slider design in terms of frictional power loss.

2 Overall mechanical efficiency prediction methodology

The HGM engine incorporates elements that represent a challenge for the designer in being either sophisticated in its own design requirements or tightly constrained due to engine size limitation. These challenges require the designer to run different design scenarios for the engine to ensure the final design satisfies the engine characteristics required. Figure 2 illustrates the overall technical methodology used in this study for the prediction of the mechanical efficiency of the HGM engine. It consists of four main components: (i) design of HGM engine components, (ii) HGM friction model, (iii) HGM and conventional engines power losses model, and (iv) mechanical efficiency computation formulation of HGM and conventional engines. The gearing and bearing design models use the engine specifications to size the required gears and bearings and predict load and contact pressure distributions at every contact point at each incremental mesh position. Predicted load and contact pressure distributions together with geometry, kinematic parameters, surface finish, and lubricant parameters are input to a friction model to predict the engine's frictional power losses. The HGM engine mechanical efficiency methodology will be validated by using the friction model of the conventional crank-slider engine [1]. The main components of this methodology, as shown in Fig. 2, are described in the following sections.

3 Hypocycloid gear engine

Figure 3 shows the detailed design of the planetary crank gear system that is utilizing the principle of the HGM for one-cylinder engine [14]. It consists of two identical gear sets mounted back-to-back, with enough space between them to allow room for the crank pin. Each gear set consists of three basic components commonly known as an internal ring gear, two planet pinion gears, and a planet pinion carrier, respectively. The internal ring gear is attached to the crankcase portion of the engine block and does not rotate with respect to the other rotating members. The planet pinion carrier is

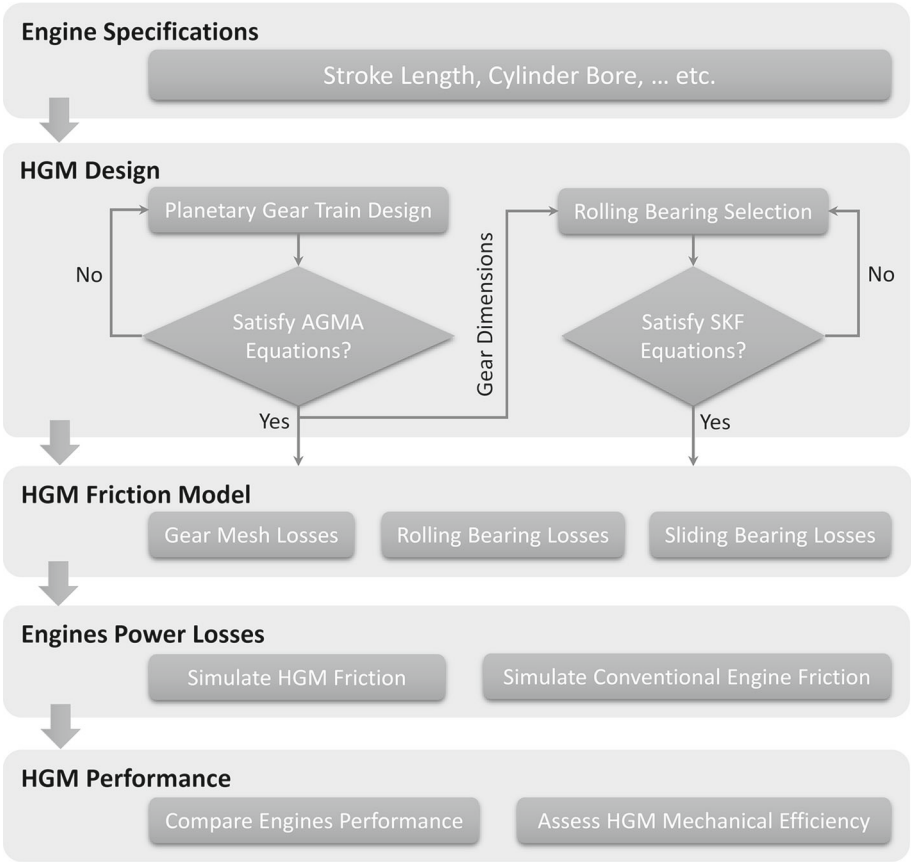

Fig. 2 HGM interactive design methodology

mounted on the inside of the rolling bearing which is allowed to rotate freely. With this arrangement, as the planet carrier is rotated 360°, the crank pin journal within one end of the connecting rod reciprocates up and down in a linear motion across the pitch diameter of the fixed internal ring gear.

The position of the centerline of the driving lug is offset by driving lug offset (δ) from the centerline of the crankshaft. The driving lugs with their sliding bearings are then indexed into a slot in a driven disk. The shaft portion of the driven disk is supported by bearings that are mounted in the lower crankcase portion of the engine block. The power output torque of the engine is taken from the shaft portion of the driven disk. When the crankshaft rotates, the driving lug orbits around the center of rotation of the pinion shaft. As the entire planetary crank assembly is rotated 360°, the path of the driving lug is an ellipse, as shown in Fig. 4. The radius of this path $r(\theta)$, Eq. (1), is determined by the engine stroke length (S) and the amount of offset of the driving lug (δ).

$$r(\theta) = \frac{(0.25S + \delta)(0.25S - \delta)}{\sqrt{(0.25S + \delta)^2 sin^2\theta + (0.25S - \delta)^2 cos^2\theta}} \quad (1)$$

For a zero offset (δ), the centerlines of the crankshafts will be coincident with the respective centerlines of driving lugs. As a result, the path of the driving lugs with no offset will be a circular path, as shown in Fig. 4. Due to the fact that the polar radius of the elliptical orbit $r(\theta)$ varies from minor to major radii (a, b), the length of the semi-major axis will be the maximum moment arm offered by the crankshaft where the output shaft is at 90° after top dead center. This characteristic also provides a nonlinear rate of piston movement because of the elliptical path of driving lugs around the axis of the output shaft, which caused the piston movement near the ends of a stroke to be slower to provide additional time for combustion operation.

Now, with the concept of HGM clearly defined, the biggest concern about the mechanism was the ability of internal gear train to withstand ICE loads. Therefore, the next section will handle this concern to ensure the mechanism is safe from strength point of view. Afterwards, the interaction between the engine elements should be assessed in terms of frictional losses to estimate the power losses of the HGM engine.

4 Planetary crank gearing system design

Due to the straight-line formed by the piston-rod motion, the gas force acting on the piston head (F_g) is aligned with the cylinder axis so that the tendency for the piston to move transversely and tilt is totally eliminated. The gas force is

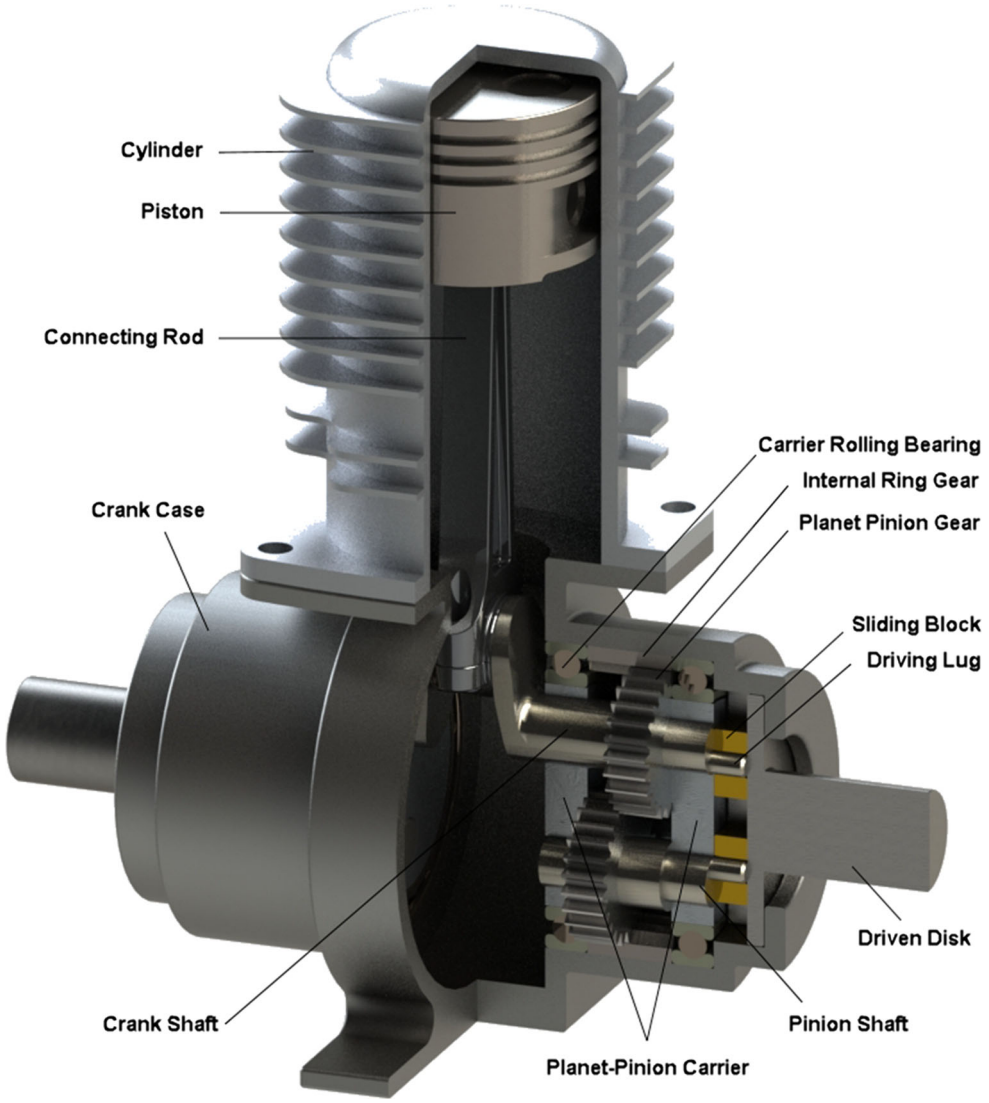

Fig. 3 Sectional assembly view of the single cylinder and associated HGM assembly

completely transmitted from the piston by the connecting rod to the crank pin center causing the crankshaft to rotate. As the planet pinion rotates around the crankshaft axis and is in continuous engagement with the internal ring gear, the tangential gear tooth load on the planet pinion, given in Eq. (2), is found to be a function of the gas force and independent of the engine speed, where L_C is the crank length.

$$F_t(\theta) = F_g(\theta)\left(\frac{r(\theta)}{L_C + \delta}\sin\theta\right) \tag{2}$$

Hypocycloid gear teeth should be designed with a load carrying capacity greater than the peak tangential force found from Eq. (2). Due to the kinematics of the HGM engine, the peak tangential force does not necessarily occur at TDC as the peak gas force. For this reason, gear teeth should be able to withstand the peak tangential force at any angular position of the crank. The design procedure for the hypocycloid gear is carried out based on AGMA standard [15].

4.1 Hypocycloid gear sizing

The AGMA standard design procedure provides two fundamental formulas for rating gears. The first formula, given by Eq. (3), should be used to make sure that progressive pitting is not going to occur to the hypocycloid gear teeth surface during the engine design life time.

$$s_c = C_p\sqrt{F_t K_o K_v K_s \frac{K_m}{dF}\frac{C_f}{I}} \le \frac{s_{ac}}{S_H}\frac{Z_N}{K_T}\frac{C_H}{K_R} \tag{3}$$

where s_c is the contact stress number and C_p is the elastic coefficient. K_o, K_v, K_s, K_m, and C_f are factors that consider gear overload, dynamic effects, gear size, teeth load distri-

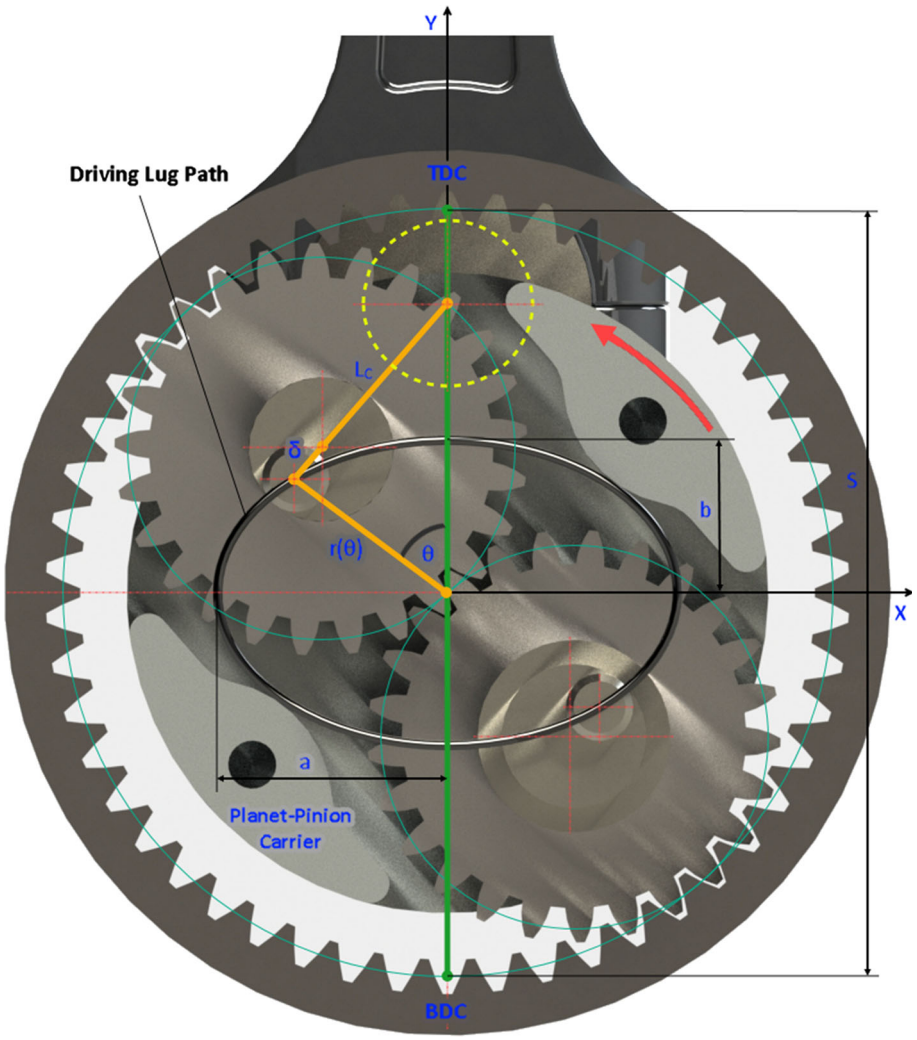

Fig. 4 Kinematic scheme of the HGM

bution, and surface condition, respectively. F_t is the peak tangential gear tooth load, as calculated from Eq. (2), and I is the pitting resistance geometry factor. The variables d and F are gear pitch diameter and face width, respectively. The contact stress shouldn't exceed the allowable stress where s_{ac} is the allowable contact stress number, S_H is the safety factor for pitting resistance, and Z_N, K_T, C_H, and K_R are factors that consider applied stress cycle, operating temperature, gear pair hardness ratio, and design reliability, respectively.

The second formula, given by Eq. (4), is used to ensure that the transmitted peak tangential force on the hypocycloid gear tooth is not going to cause tooth-bending failure during the engine design life time.

$$s_t = F_t K_o K_v K_s \frac{P_d}{F} \frac{K_m K_B}{J} \leq \frac{s_{at} Y_N}{S_F K_T K_R} \tag{4}$$

where s_t is the bending stress number, P_d is the diametral pitch, K_m is the rim thickness factor, and J is the bending strength geometry factor. Similarly, bending stress number should not exceed the allowable stress where s_{at} is the allowable bending stress number, S_F is safety factor for bending strength, and Y_N is stress cycle factor.

AGMA also provides two power rating formulas which should be used as a check to make sure that the transmitted power by the hypocycloid gears doesn't exceed the allowable power to avoid tooth surface pitting, Eq. (5), or the allowable power to avoid tooth bending failure, Eq. (6), during the engine design life time.

$$P_{ac} = \frac{\pi n_p F}{396{,}000} \frac{I}{K_o K_v K_s K_m C_f} \left(\frac{d s_{ac}}{C_p S_H} \frac{Z_N C_H}{K_T K_R} \right)^2 \tag{5}$$

$$P_{at} = \frac{\pi n_p d}{396{,}000 K_o K_v} \frac{F}{P_d} \frac{J}{K_s K_m K_B} \frac{s_{at} Y_N}{S_F K_T K_R} \tag{6}$$

where P_{ac} and P_{at} are the allowable transmitted power for pitting resistance and for bending strength, respectively. The variable n_p is the speed of planet pinion gear.

4.1.1 Geometry factors

It is recommended that the geometry factors, I and J, used in the fundamental rating equations to be determined using the recommended procedure of AGMA [16]. For the pitting resistance geometry factor (I), it is evaluated using Eq. (7).

$$I = \frac{\cos\phi C_{\psi}^2}{\left(\frac{1}{\rho_1} \pm \frac{1}{\rho_2}\right) dm_N} \tag{7}$$

where the $\pm$ sign here and afterwards is to indicate external gearing (+) and internal gearing (−), ϕ is the operating pressure angle, C_{ψ} is the helical overlap factor, ρ_1 and ρ_2 are the curvature radius of pinion and gear tooth profile, respectively, and m_N is the load sharing ratio.

For the bending strength geometry factor (J), it can be evaluated using Eq. (8) for external gears only, where Y is the tooth form factor, K_f is the stress concentration factor. For internal gears, the model presented in Annex A of AGMA aerospace gearing design [17] will be utilized. Despite the fact that the internal gear model is for spur gear meshes only, helical gears can be preliminarily estimated such that the resulting value can serve as the starting point for a detailed finite element analysis afterward.

$$J = \frac{YC_{\psi}}{K_f m_N} \tag{8}$$

For internal gears, the main idea is that it is required to determine the size of the largest inscribed parabola in the internal gear tooth. Based on the size of this parabola, the critical tooth section is defined then the geometry factor is established and can be calculated using Eq. (9).

$$J = \frac{1}{K_f \frac{\cos\phi_n}{\cos\phi}\left[\frac{6h}{t^2} - \frac{\tan\phi_n}{t}\right]} \tag{9}$$

where ϕ_n is the angle of tooth profile normal force. The two variables h and t are the parabola height and thickness, both measured at the tooth critical section for the minimum geometry factor.

Once the hypocycloid gear size satisfies standard AGMA design constraints, therefore the planetary gear size used is ensured to withstand the ICE requirements. So, the following step would be, based on the size of the planetary gears (diameters and face width) and the gas force generated, the carrier rolling bearing required can be selected and then the friction between engine components can be analyzed.

5 HGM engine frictional power losses

The HGM engine has an increased number of friction interfaces compared to a conventional crank-slider engine due to additional bearings and gear meshes. Thus, the frictional losses for these components are an important concern that should be analyzed to ensure that HGM friction losses are not exceeding the conventional crank-slider losses. In this section, frictional power loss models will be developed for gear meshes, rolling bearings, and sliding bearings.

5.1 HGM gear mesh losses

Since gears are the primary power transmission component in this design, power losses caused by the gear set are critical to the overall power transmission efficiency of the HGM engine. Power losses in any geared transmission can be classified into two main categories [18, 19]: load-dependent (mechanical) power losses and load-independent (spin) power losses. Load-dependent power losses result from the relative sliding and rolling action of an elastohydrodynamic lubricant film between meshing teeth. Load-independent power losses can result from the drag of rotating components and pocketing of lubricant at the gear mesh interface. Depending on the input power and speed, lubricant characteristics, and crankcase design, the load-independent gear power losses are usually a very important source of power loss. Due to an almost infinite combination of crank case design choices and operating conditions, it is very difficult to develop a simple and general formulation to evaluate these power loss mechanisms. For this reason, the gear set load-independent power loss needs to be measured from experimental observations for reliable power loss values.

The mechanical power loss calculations for the geared hypocycloid engine design with pinion/internal gear pair can utilize the *Ohlendorf* method [20, 21] and the Velex et al. method [22, 23]. These methods are known to be applicable with planetary gear trains, so both external and internal gearing power losses can be assessed.

5.1.1 Ohlendorf equation

The power loss generated between meshing hypocycloid gear teeth can be calculated according to Eqs. (10, 11), where P_{VZP} is the load-dependent gear power loss, P_{IN} is the input power, H_V^{ohl} is the gear loss factor, and μ is the friction coefficient.

$$P_{VZP} = P_{IN} H_V^{ohl} \mu \tag{10}$$

$$H_V^{ohl} = \left(\frac{u \pm 1}{u}\right) \frac{\pi}{z_1} \frac{1}{\cos\beta_b} \left(1 - \epsilon_\alpha + \epsilon_1^2 + \epsilon_2^2\right) \tag{11}$$

where u is the gear ratio, z_1 is the pinion number of teeth, β_b is the helix angle measured at the base circle. The variables $\in_\alpha$, $\in_1$, and $\in_2$ are the transverse, addendum, and dedendum contact ratios, respectively.

5.1.2 Velex et al. equation

The efficiency of a meshing hypocycloid gear pair was obtained as a closed form solution, as presented in Eqs. (12–14), where ρ is gear pair efficiency, $\Lambda(\mu)$ is a dimensionless loss factor, and K_o is a dimensionless factor related to pitch point position on base plane.

$$\rho = 1 - \mu\left(\frac{u \pm 1}{u}\right)\frac{\pi}{z_1}\frac{1}{\cos\beta_b}\epsilon_\alpha \Lambda(\mu) \tag{12}$$

$$\Lambda(\mu) = \frac{2k_o^2 - 2k_o + 1}{1 - \mu\left(\frac{\tan\phi(2k_o - 1) - \frac{\pi}{z_1}\epsilon_\alpha\left(k_o^2 - 2k_o + 1\right)}{\cos\beta_b}\right)} \tag{13}$$

$$K_o = \frac{z_1 u}{2\pi\epsilon_\alpha}\left(\pm\sqrt{\left(\frac{r_{a_2}}{r_{p_2}}\right)^2\frac{1}{cos^2\phi} - 1} \mp \tan\phi\right) \tag{14}$$

where r_{a2} is the gear addendum radius and r_{p2} is the gear pitch radius.

Since the Ohlendorf equation was reported to give very close results to elasticity solution of finite element software packages [20], the authors will be utilizing this equation for the HGM engine friction model.

5.1.3 Friction coefficient

As seen in Eq. (10), power loss calculation requires the knowledge of the frictional coefficient between meshing gear teeth surfaces. The coefficient of friction depends on gear materials, accuracy of tooth form, surface finish condition, lubrication, sliding velocity, and surface stress condition. The mean coefficient of gear tooth friction can be approximated using the *Schlenk's Equation* [19, 20]. Assuming that the average coefficient of friction (μ_{mZ}) is constant along the path of contact, it then can be calculated from Eq. (15).

$$\mu_{mz} = 0.048\left(\frac{F_{bt}/F}{V_{\Sigma C}\rho_C}\right)^{0.2}\eta_{oil}^{-0.05}R_a^{0.25}X_L \tag{15}$$

where F_{bt} is the tangential gear force calculated at base plane, $V_{\Sigma C}$ is the sum velocity at the pitch point, ρ_C is the equivalent contact radius at the pitch point, and R_a is the average roughness for the gear tooth. The variable η_{oil} is the lubricant dynamic viscosity, and X_L is a lubricant parameter.

This equation was derived from experiments for mineral oils without additives with the lubricant factor (X_L) equals 1.0 for mineral oils. When different gear oil formulations are considered, the X_L coefficient must be adjusted to account for the influence of different base oils and/or additive packages.

5.2 Rolling bearings power losses

Similar to gears, rolling bearing power losses can be classified into load-independent and load-dependent losses. The total resistance to rotation in a rolling bearing is the result of rolling and sliding friction in the contact areas, between the rolling elements and raceways, between the rolling elements and cage, and between the rolling elements and other guiding surfaces. Friction is also generated by lubricant drag and by contact seals, if applicable. For the HGM engine rolling bearings friction model, this study will utilize the friction torque model developed by the SKF [24].

The SKF model for calculating the frictional moment closely follows the real behavior of the bearing as it considers all contact areas, design changes and improvements made to SKF bearings as well as internal and external influences. The total frictional moment (M) of the carrier rolling bearing can be calculated utilizing Eq. (16) given below. The four terms represent the rolling (M_{rr}) and sliding (M_{sl}) friction moments, friction moment of seals (M_{seal}), and the drag losses (M_{drag}), respectively.

$$M = M_{rr} + M_{sl} + M_{seal} + M_{drag} \tag{16}$$

The rolling frictional moment (M_{rr}) can be calculated using Eqs. (17–19), where ϕ_{ish} is the inlet shear heating reduction factor, ϕ_{rs} is the kinematic replenishment/starvation reduction factor. The constant G_{rr} is the rolling friction variable, calculated from SKF tables based on bearing type, size, and loads.

$$M_{rr} = \phi_{ish}\phi_{rs}G_{rr}(vn)^{0.6} \tag{17}$$

$$\phi_{ish} = \frac{1}{1 + 1.84 \times 10^{-9}(nd_m)^{1.28}v^{0.64}} \tag{18}$$

$$\phi_{rs} = \frac{1}{e^{\left[K_{rs}vn(d+D)\sqrt{\frac{K_Z}{2(D-d)}}\right]}} \tag{19}$$

where v is the actual operating viscosity of the lubricant, n is the carrier rotational speed. The variables d, d_m, and D are the bearing bore, mean, and outside diameters, respectively. K_{rs} is the replenishment/starvation constant, calculated from SKF based on lubrication type, and K_Z is a geometric constant, calculated by SKF based on bearing type.

The sliding frictional moment (M_{sl}) can be calculated using Eq. (20–22) where μ_{sl} is the sliding friction coefficient and ϕ_{bl} is a weighting factor. The constant G_{sl} is the sliding friction variable calculated from SKF tables based on bearing type, size, and loads.

$$M_{sl} = G_{sl}\mu_{sl} \tag{20}$$

$$\mu_{sl} = \phi_{bl}\mu_{bl} + (1 - \phi_{bl})\mu_{EHL} \tag{21}$$

$$\phi_{bl} = \frac{1}{e^{2.6\times10^{-8}(n\nu)^{1.4}d_m}} \tag{22}$$

where μ_{bl} is a coefficient calculated by SKF recommended value depending on the additive package in the lubricant. μ_{EHL} is the sliding friction coefficient in full-film condition, calculated based on SKF recommended values.

As for friction moment of seals (M_{seal}), the frictional losses from the seals may exceed those generated by the bearing. For the HGM engine, the authors are considering the selection of bearings without contact seals since the entire crankcase is expected to be lubricated using the same lubricant. Therefore, this term is disregarded in HGM friction model.

Similar to gears, drag losses (M_{drag}) that occur when the bearing is rotating in an oil bath contribute to the total frictional moment and should not be neglected. Drag losses are not only influenced by bearing speed, oil viscosity, and oil level, but also by the size and geometry of the oil reservoir. Since at this point there is no detailed design for the HGM engine crankcase, this term is disregarded too in HGM friction model.

The power loss in the carrier rolling bearing (N_R) because of bearing friction can then be estimated using Eq. (23).

$$N_R = 1.05 \times 10^{-4} Mn \tag{23}$$

5.3 Sliding bearings power losses

By analyzing the HGM engine, the design uses a plain journal bearing with concentric cylinders, and a sliding block with planer contact surface. Under conditions of hydrodynamic lubrication, the sliding bearings surfaces are separated by a relatively thick film of fluid lubricant, and the normal load is supported by the pressure within this film, which is generated hydrodynamically [25]. The gap between the two bearing surfaces is filled with the lubricating fluid where the separations of the surfaces and the angles of convergence are typically very small. A plain journal bearing lubricated with oil will have a mean lubricant film thickness of the order of one thousandth of the journal diameter, while the maximum and minimum film thicknesses may differ by a factor of four or five [26].

5.3.1 Driving lug

The load per unit width (W_{DL}) for the driving lug can be calculated using Eqs. (24–26), where S is a dimensionless number, the *Sommerfeld Number*, which is determined by the width (w) to diameter (D) ratio for the bearing and by the eccentricity ratio (ε) of the driving lug within the sliding block.

$$W_{DL} = S\eta U\left(\frac{R^2}{h^2}\right) \tag{24}$$

$$S = \left(\frac{w}{D}\right)^2 \frac{\pi\varepsilon}{\left(1-\varepsilon^2\right)^2}\sqrt{0.621\varepsilon^2 + 1} \tag{25}$$

$$\varepsilon = \frac{e}{c} = \frac{(h_1 - h_o)/2}{(h_1 + h_o)/2} \tag{26}$$

where η is the dynamic viscosity of the lubricant used, U is the sliding velocity at the driving lug circumference, R is the driving lug radius. Variables e and c are the eccentricity and the mean radial clearance, respectively. Constants h_o, h, and h_1 are minimum, mean, and maximum film thickness (radial clearance), respectively.

The total frictional tangential force per unit width (F_{DL}) acting on the periphery of the driving lug is given to a good approximation for an infinitely wide bearing by the *Petrov* Eq. (27) below. Then, the mean coefficient of friction (μ_{DL}) for the driving lug can be approximated as given by Eq. (28).

$$F_{DL} = 2\pi\eta U\frac{R}{h} \tag{27}$$

$$\mu_{DL} = \frac{F_{DL}}{W_{DL}} = \left(\frac{2\pi}{S}\right)\left(\frac{h}{R}\right) \tag{28}$$

Therefore, the power loss $(hp_{DL})_{loss}$ for driving lug is calculated as;

$$(hp_{DL})_{loss} = \frac{T_{DL,f}N}{1{,}050} \tag{29}$$

where $T_{DL,f}$ is the frictional torque on the driving lug and N is the driving lug rotational speed.

5.3.2 Sliding block

The load per unit width (W_{SB}) for the sliding block can be calculated using Eqs. (30–32), where L is the sliding block length and K is a factor whose value depends on the ratio of the inlet and outlet film thicknesses only.

$$W_{SB} = 6\eta K U\left(\frac{L^2}{h_o^2}\right) \tag{30}$$

$$K = \frac{\ln(1+n)}{n^2} - \frac{2}{n(2+n)} \tag{31}$$

$$n = \frac{h_1}{h_o} - 1 \tag{32}$$

In a similar manner for *Pertov Equation*, the frictional force for the sliding block can also be predicted. The total frictional tangential force per unit width (F_{SB}) acting on the periphery of the sliding block is given to a fair approximation

by Eq. (33) below. Then, the mean coefficient of friction (μ_{SB}) for sliding block can be approximated as given by Eq. (34).

$$F_{SB} = \eta U \frac{L}{h} \tag{33}$$

$$\mu_{SB} = \frac{F_{SB}}{W_{SB}} = \frac{h}{6LK} \times 1.8 \tag{34}$$

The constant 1.8 used in Eq. (34) was added to account for the mixed lubrication regime of the sliding block, since the operation of the sliding block requires it to reciprocate along the driven disk, as shown in Fig. 3. At the end of the reciprocating length, the lubrication regime is expected to be boundary lubrication, while at the middle where the block is having a maximum speed, the lubrication is hydrodynamic. Therefore, as an approximation for such lubrication condition, the authors are using the 1.8 constant as suggested by Sandoval and Heywood [1].

Therefore, the power loss for the sliding block $(hp_{SB})_{loss}$ is calculated as;

$$(hp_{SB})_{loss} = \frac{F_{SB} V_{SB,s}}{6{,}600} \tag{35}$$

$$V_{SB,s} = \omega \times r(\theta) \tag{36}$$

where $V_{SB,\,S}$ is the block sliding velocity and ω is the angular speed of the driven disk.

At this point, the friction model for HGM engine is completely developed. The main aim is to assess the performance of HGM engine in terms of frictional power losses, and then compare its performance with the conventional crank-slider engine to validate the minimized frictional losses of the new design. Therefore, the last step of friction modeling is to introduce the model used with conventional engines, which will be discussed in the next section.

6 Conventional engine friction model

The model proposed by Sandoval and Heywood [1, 27, 28] which was based on a combination of fundamental scaling laws and empirical results, will be utilized for this study. It includes predictions of friction losses for spark ignition engines, where the losses are classified into three main categories: mechanical (rubbing) losses, pumping losses, and auxiliary component losses. Mechanical losses result from relative motion between solid interacting surfaces in the engine, for example the motion between a piston ring and a cylinder wall, or a crankshaft journal in a bearing. Pumping losses are the work done by the piston as gases are pushed out of and pulled into the cylinder during the exhaust and intake strokes since it is considered flow resistance for naturally aspirated engines. Auxiliary component losses are the work required to drive essential engine accessories, for example the fans, pumps, and air conditioning.

For the purpose of HGM friction assessing, the authors are considering only a part of the mechanical losses, which is the reciprocating elements friction. This includes piston skirt, piston ring, and connecting rod friction. Piston ring friction was divided into two terms; one that predicted friction for the piston rings without gas pressure loading, and one that predicted the increase in piston ring friction caused by gas pressure loading. The term for the connecting rod's bearing losses was disregarded since it exists also in HGM engine. The formulas below can be used to estimate the piston friction losses in terms of frictional mean effective pressure.

The reciprocating friction mean effective pressure (*rfmep*) can be estimated using Eq. (37).

$$rfmep = 2.94 \times 10^2 \sqrt{\frac{\mu}{\mu_o}} \left(\frac{S_p}{B}\right) + 4.06 \times 10^4 \left(\frac{F_t}{F_{to}} C_r\right) \left(1 + \frac{500}{N}\right) \left(\frac{1}{B^2}\right) \tag{37}$$

where μ is operating oil viscosity, μ_o is the reference oil viscosity, S_p is the piston speed, B is cylinder bore, F_t/F_{to} is piston ring tension ratio, C_r is the piston roughness ratio, and N is the engine speed.

The first term in Eq. (37) represents piston skirt friction assuming hydrodynamic lubrication while the second term represents piston ring friction under mixed lubrication. When the gas force application is considered, the increase in piston ring friction losses ($rfmep_{gas}$) can be estimated using Eq. (38).

$$rfmep_{gas} = 6.89 \frac{p_i}{p_a} \left[0.088 \sqrt{\frac{\mu}{\mu_o}} r_c + 0.182 \left(\frac{F_t}{F_{to}}\right) r_c^{(1.33 - 2KS_p)}\right] \tag{38}$$

where p_i and p_a are the intake-manifold and atmospheric pressures, respectively, r_c is the compression ratio, and K is a constant with a value of 2.38×10^{-2}.

7 Model validation

The developed friction model is assessed using one selected vehicle engine from the market, utilizing the engine parameters available to first sizing the gears for HGM, selecting the rolling bearings to be used, and then estimating the frictional power losses. This will be followed by a comparison with the frictional power losses that would result from the conventional crank-slider engine's piston.

Table 1 Engine specifications for the selected passenger car

Engine type	Spark Ignition—4 stroke
Displacement (in^3)	91.1
Net horsepower	192 hp @ 5500 rpm
Net torque	192 lb.ft @ 1600–5000 rpm
Bore (in)	2.87
Stroke length (in)	3.52
Compression ratio	10.3

Table 2 Gear train parameters

Gear parameter	Pinion	Internal gear
Pitch circle diameter (in)	1.76	3.52
Number of teeth	18	36
Diametral pitch (in^{-1})	10.23	
Face width (in)	0.78	1.56
Pressure angle (°)	20	
Helix angle (°)	0	
Gear ratio	2	
Material	Steel, carburized and hardened—grade 2	
Brinell hardness number (HB)	300	
Contact stress number (psi)	167,300	118,300
Bending stress number (psi)	58,115	17,260

7.1 Engine parameters

For validating the developed model, one conventional engine for a passenger car is selected from the market. The specifications of the selected engine represent the design requirements and constraints for the planetary gear train, rolling and sliding bearings. Table 1 shows a summary for the selected engine specifications.

7.2 HGM engine design

Based on the engine specifications given, gear design procedures based on the AGMA standard presented in section four is carried out. Table 2 shows the dimensions of the planetary gear set satisfying engine specifications.

It should be noted here that the diametral pitch assumed for the design is a non-standard value, since the internal gear diameter (stroke length) is fixed and the number for gear teeth to be selected must be integer. Therefore, the authors are assuming there is a cutting tool that can be used to produce this size of the gear teeth. This assumption is valid since automotive industry is mass production, so it can be claimed that such a tool is available once the engine design is fixed and approved.

Table 3 Parameters of the carrier rolling bearing

Designation	Deep groove ball bearing—SKF 16014
Outside diameter (mm)	110
Mean diameter (mm)	90
Width (mm)	13
Inner race outer diameter (mm)	83.3
Basic load rating—static (N)	25,000

Rolling bearing selection is made taking in considerations two concerns; first, to make sure that the inner race is not to be in contact with the internal ring gear teeth, so it is free to rotate and unnecessary friction between rolling bearings and internal gears is avoided. The second concern is to withstand the gas force loading to be transmitted by the piston, which is the radial load to be supported by the rolling bearings. For engine and gear parameters given in Tables 1 and 2, the rolling bearing satisfying the two concerns is selected to be deep groove ball bearing—*SKF 16014* [24]. Table 3 briefly summarizes the selected rolling bearing parameters.

For HGM engine lubrication, the authors are considering gear lubricants to be the basis of viscosity grade selection. AGMA guideline procedures in Annex B for industrial gear lubrication [29] is followed to get an estimate of the required viscosity grade. The lubricant selection is based on the recommended viscosity grade for gears, which is a function of viscosity index, pitch line velocity, and operating temperature. The recommended viscosity grade selected is utilized also with the rolling and sliding bearings friction calculations assuming that the entire crankcase should utilize the same lubricant. For the conventional engine, the power loss model presented in section six is utilizing *SAE 10W30* oil grade lubricant as recommended by the model developers, since it is in the mid-range of oils used for conventional engine lubrication.

7.3 Model simulation results

Simulation of the HGM engine performance is developed using Excel to find the power loss due to friction at the major components of the engine, total power loss due to friction, and HGM engine efficiency. Simulations are carried out over the speed range of regular passenger cars for both HGM and conventional engines.

Figure 5 shows the amount of frictional power losses (load-dependent) for the planetary gear set, the rolling bearing, and the sliding bearing over the speed range for the engine. Figure 6 shows the combined frictional power losses over the speed range for the engine. The combined losses for HGM was found by considering power delivered through

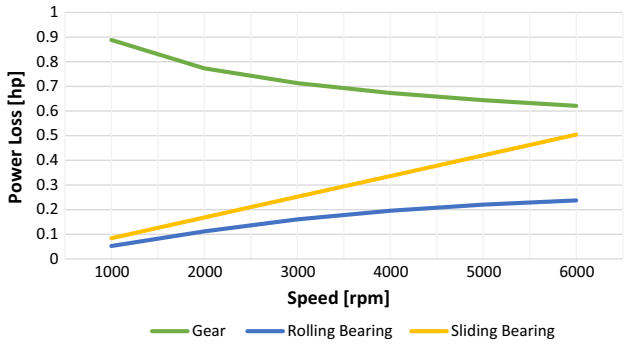

Fig. 5 HGM components power loss

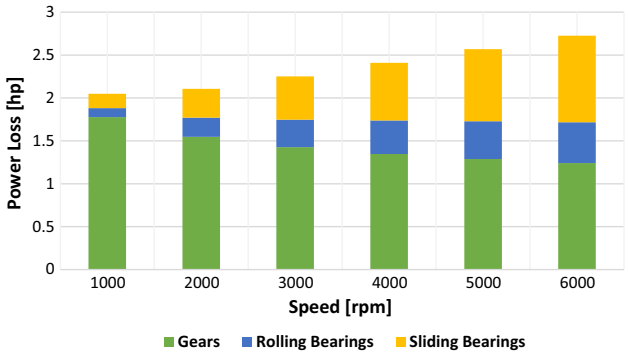

Fig. 6 HGM total power loss

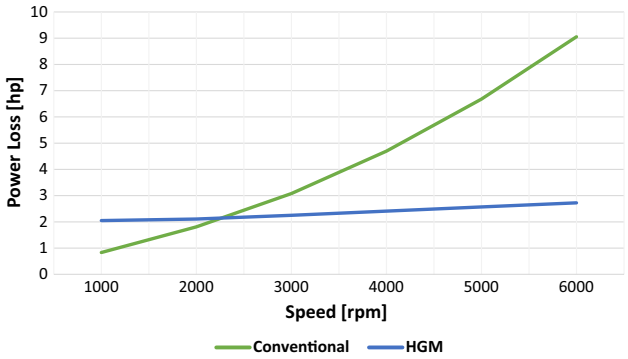

Fig. 7 HGM versus conventional piston power loss

two paths, all component of the power looses are multiplied by two.

Figure 7 is a comparison between the total frictional power losses for the HGM engine and the conventional crank-slider engine piston over the speed range of the engine. Figure 8 is a comparison between the efficiency of the HGM engine and the conventional crank-slider engine's piston over the speed range of the engine.

The simulation results show that over the speed range of motion, the frictional power losses of the HGM engine is almost constant as compared with the conventional crank-slider engine, as shown in Fig. 7. The reason for the almost steady HGM engine power loss is the balancing of the losses

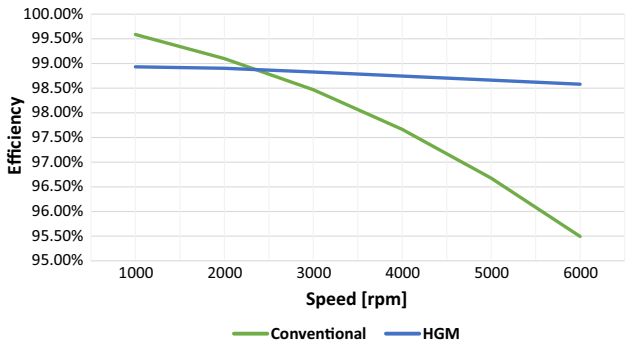

Fig. 8 HGM versus conventional piston efficiency

between the HGM engine components, as shown in Fig. 6, where at low speeds the gears have high power losses as compared with the bearings. As the speed increase, gear power losses decreases as the coefficient of friction given by Schlenk's Eq. (15) is inversely proportional with speed. On the other hand, power losses at the bearings are directly proportional with the speed, which would result on an overall HGM engine power loss that is slightly increasing with the speed.

Although Fig. 8 shows that the efficiency of the conventional crank-slider engine piston is slightly higher than that of the HGM engine at low speeds by 0.6%, the conventional engine's piston efficiency drops by 4.1% at the highest speed reaching 95.5%. In contrast, HGM engine efficiency is maintained at roughly 98.75% with a 0.35% decrease in efficiency over the entire speed range of motion.

One factor that affected the simulation results is the lubricant viscosity. The use of one lubricant in the crankcase is based on what is beneficial for gears, where the higher viscosity the lubricant is, the better efficiency gears will have [29]. In contrast, rolling and sliding bearings require less lubricant viscosities than gears for higher bearing efficiency. Therefore, there should be a compromise between the lubrication needs necessary in the crankcase for the best overall efficiency of the HGM engine.

8 Conclusions

This work has focused on the feasibility of HGM as an alternative for conventional crank-slider mechanism in ICE applications. Since the literature review showed that HGM engine considers gears as the critical components in the design, higher attention is given to gear design in this investigation to ensure that the gear tooth strength is adequate to withstand the engine's load and to satisfy all the engine's specifications.

Friction models of the interacting components in HGM engine is developed. The model for gear friction losses is

designed to be applicable with internal gear meshes where all the calculated parameters satisfy the internal gear set specifications and geometries. The lubricant viscosity grade is selected based on the recommendations and guidelines provided by AGMA for gear meshes. For bearing losses, the SKF friction torque model is utilized to estimate the frictional power losses of the carrier's rolling bearing while the sliding bearings friction model is approximated from tribology and machine elements design handbooks for both the journal type and the planer-sliding type.

The validity of the developed friction model for HGM engine is assessed against the conventional crank-slider engine through selecting one passenger car's conventional engine, utilizing its parameters to size the components of the HGM engine, and then estimating the frictional power losses and efficiencies for both engines over the engine speed range. The analysis done in this paper shows promising results for the HGM engine performance data in terms of minimized frictional power losses, hence higher engine mechanical efficiency that is maintained over the speed range of the engine. The main concern about HGM engine complexity, variety of components, and many frictional interfaces is proven to result in minimum losses as compared with the benefits of eliminating the conventional engine piston side thrusting.

The future work is to investigate engines with higher speeds and/or power generation, check the feasibility of using spur/helical gears to transmit such higher powers and/or speeds. Also, deciding on what lubricant should be selected for minimizing friction losses, and satisfy gear meshing requirements. Also, it is to investigate the effect of the lubrication method and crank case design on the load-independent power losses for gears and rolling bearings. Finally, to validate all these results through some experimental testing of a prototype for HGM.

References

1. Sandoval, D., Heywood, J.B.: An Improved Friction Model for Spark-Ignition Engines. SAE Technical Paper 2003-01-0725 (2003)
2. Sethu, C., Leustek, M.E., Bohac, S.V., Filipi, Z., Assanis, D.N.: An Investigation in Measuring Crank Angle Resolved In-Cylinder Engine Friction Using Instantaneous IMEP Method. SAE Technical Paper 2007-01-3989 (2007)
3. Richardson, D.E.: Review of power cylinder friction for diesel engines. ASME J. Eng. Gas Turbines Power **122**, 506–519 (2000)
4. Hoshi, M., Baba, Y.: A Study of Piston Friction Force in an internal combustion engine. ASLE Trans. **30**, 444–451 (2008)
5. Nagar, P., Miers, S.: Friction Between Piston and Cylinder of an IC Engine: A Review. SAE Technical Paper 2011-01-1405 (2011)
6. Beachley, N.H., Lenz, M.A.: A Critical Evaluation of the Geared Hypocycloid Mechanism for internal combustion engine Application. SAE Technical Paper 880660 (1988)
7. Ruch, D.M., Fronczak, F.J., Beachley, N.H.: Design of a Modified Hypocycloid Engine. SAE Technical Paper 911810 (1991)
8. Burkett, M.J., Beachley, N.H., Fronczak, F.J.: Lubrication Aspects of a Modified Hypocycloid Engine. SAE Technical Paper 920380 (1992)
9. Karhula, J.: Cardan Gear Mechanism versus Slider-Crank Mechanism in Pumps and Engines. Ph.D. dissertation, Lappeenranta University of Technology (2008)
10. Ray, P., Redkar, S.: Analysis and simulation of Wiseman hypocycloid. Cogent Eng. **1**, 988402 (2014)
11. Badami, M., Andriano, M.: Design, Construction and Testing of Hypocycloid Machines. SAE Technical Paper 980120 (1998)
12. Rucker, R.D.: An Analysis of the Parallel Combustion Two-Stroke Engine. SAE Technical Paper 2000-01-1022 (2000)
13. Haynes, M.W., Aziz, E.S., Chassapis C.: Planetary Crank Gear Design for Internal Combustion Engines. Patent US9540994B2 (2017)
14. Aziz, E.S., Chassapis, C.: Enhanced hypocycloid gear mechanism for internal combustion engine applications. ASME J. Mech. Des. **138**, 125002 (2016)
15. American National Standard: Fundamental Rating Factors and Calculation Methods for Involute Spur and Helical Gear Teeth. American Gear Manufacturers Association, Alexandria (2004)
16. AGMA Information Sheet: Geometry Factors For Determining the Pitting Resistance and Bending Strength of Spur, Helical and Herringbone Gear Teeth. American Gear Manufacturers Association, Alexandria (1989)
17. AGMA Information Sheet: Design Guidelines for Aerospace Gearing. American Gear Manufacturers Association, Alexandria (1994)
18. Talbot, D.C., Kahraman, A., Singh, A.: An experimental investigation of the efficiency of planetary gear sets. ASME J. Mech. Des. **134**, 021003 (2012)
19. Höhn, B.-R., Michaelis, K., Vollmer, T.: Thermal Rating of Gear Drives: Balance Between Power Loss and Heat Dissipation. AGMA Technical Paper 96FTM8 (1996)
20. Fernandes, C.M., Marques, P.M., Martins, R.C., Seabra, J.H.: Gearbox power loss. Part II: friction losses in gears. Tribol. Int. **88**, 309–316 (2015)
21. Moldovean, G., Butuc, B.R., Bozan, C.A.: On the power losses of cylindrical and bevel gears used in wind turbines and tracking systems for photovoltaic platforms. In: SYROM 2009: Proceedings of the 10th IFToMM International Symposium on Science of Mechanisms and Machines (2009)
22. Velex, P., Ville, F.: An analytical approach to tooth friction losses in spur and helical gears—influence of profile modifications. ASME J. Mech. Des. **131**, 101008 (2009)
23. Durand de Gevigney, J., Ville, F., Changenet, C., Velex, P.: Tooth friction losses in internal gears: analytical formulation and applications to planetary gears. J. Eng. Tribol. **227**, 476–485 (2013)
24. SKF 10000/3 EN: Rolling Bearings Catalogue. SKF Group, Gothenburg (2016)
25. Budynas, R.G., Nisbett, J.K.: Shigley's Mechanical Engineering Design, 10th edn. McGraw-Hill Education, New York City (2015)
26. Hutchings, I., Shipway, P.: Tribology: Friction and Wear of Engineering Materials, 2nd edn. Butterworth-Heinemann, Oxford (2017)
27. Heywood, J.B.: Internal Combustion Engine Fundamentals, 1st edn. McGraw-Hill, New York City (1988)
28. Patton, K.J., Nitschke, R.C., Heywood, J.B.: Development and Evaluation of a Friction Model for Spark-Ignition Engines. SAE Technical Paper 890836 (1989)
29. American National Standard: Industrial Gear Lubrication. American Gear Manufacturers Association, Alexandria (2016)